TITLE:

Magnetic Field Drifts of Small HTS Dipole Magnet Under Repeated Excitation

AUTHOR(S):

Sogabe, Yusuke; Wakabayashi, Koki; Amemiya, Naoyuki

CITATION:

Sogabe, Yusuke ...[et al]. Magnetic Field Drifts of Small HTS Dipole Magnet Under Repeated Excitation. IEEE Transactions on Applied Superconductivity 2022, 32(4): 4600305.

ISSUE DATE:

2022-06

URL:

http://hdl.handle.net/2433/270111

RIGHT:

© 2022 IEEE. Personal use of this material is permitted. Permission from IEEE must be obtained for all other uses, in any current or future media, including reprinting/republishing this material for advertising or promotional purposes, creating new collective works, for resale or redistribution to servers or lists, or reuse of any copyrighted component of this work in other works.; This is not the published version. Please cite only the published version. この論文は出版社版でありません。引用の際には出版社版をご確認ご利用ください。

京都大学学術情報リポジトリ
KURENAI 紅
Kyoto University Research Information Repository

京都大学 KYOTO UNIVERSITY #404
A Self-archived copy in
Kyoto University Research Information Repository
https://repository.kulib.kyoto-u.ac.jp
京都大学学術情報リポジトリ KURENAI 紅 Kyoto University Research Information Repository

Magnetic Field Drifts of Small HTS Dipole Magnet under Repeated Excitation

Yusuke Sogabe, *Member, IEEE*, Koki Wakabayashi, Naoyuki Amemiya, *Senior Member, IEEE*

***Abstract*—Shielding-current-induced fields (SCIFs) in magnets wound with coated conductors deteriorate the field quality of the magnets. Particularly, in magnets that are excited repeatedly, and must generate time-varying magnetic fields, for example, in certain types of accelerator magnets, the influence of the temporal behavior of the SCIFs on magnetic field is quite complicated. We focused on the magnetic field drifts and conducted magnetic field measurements using a small dipole magnet wound with coated conductors cooled using a cryocooler. The magnet was operated under various patterns of excitation, and magnetic fields were measured using a rotating pickup coil, which enabled us to measure the dipole and sextupole components of the magnetic field. Numerical electromagnetic field analyses were conducted to examine the current distributions in conductors, which influenced the temporal behavior of the magnetic field.**

***Index Terms*—Accelerator magnet, coated conductor, electromagnetic field analysis, field quality, shielding-current-induced field**

I. Introduction

ACCELERATOR magnets are interesting targets for high-temperature superconducting (HTS) applications [1-5]. Magnets using coils wound with coated conductors are expected to enable operation with conduction cooling without a refrigerant. Furthermore, they are capable of generating extremely high magnetic fields. However, coated conductors are strongly magnetized due to their tape shape, therefore, shielding-current-induced fields (SCIFs) complicate behaviors of magnetic fields generated using coils wound with coated conductors [6-9].

We have been studying the applications of coated-conductor magnets in rotating gantries, which are a part of carbon cancer therapy systems. Magnets in the rotating gantries are required to generate a relatively low, but stable and reproducible field. Particularly, their magnetic fields must be kept constant for short time periods like *steps* during the ramp-down process, to precisely irradiate the heavy-ion beam with a specific energy to a patient [10]. Additionally, the period of one cycle of excitation (from ramp-up to ramp-down of the magnetic field) is a few minutes, which is shorter than that of a magnet in a typical accelerator used in high-energy physics [2, 8]. There haven't been any experimental studies on the extremely complex influence of SCIFs on the field quality of magnets using coils wound with coated conductors, operated under aforementioned conditions; and only a few studies have been conducted using numerical analyses [7].

We conducted magnetic field measurements on a small HTS dipole magnet to evaluate the behavior of the SCIF during repeated excitation. Specifically, we focused on the effect on the magnetic field generated during the ramp-down process, when the current is kept constant for 10 s (to simulate the *steps* of magnetic fields, of the magnets in the rotating gantries), as the ramp-up and ramp-down processes are repeated. Hence, we evaluated the drift of the magnetic field during repeated excitation. Moreover, numerical electromagnetic field analyses were conducted to visualize the electromagnetic field distribution in the coated conductors during repeated excitation.

Manuscript receipt and acceptance dates will be inserted here. This work was supported by JSPS KAKENHI Grant Numbers JP19K23513 and JP20H00245. *(Corresponding author: Naoyuki Amemiya.)*

The authors are with the Department of Electrical Engineering, Kyoto University, Kyoto 615-8510, Japan (e-mail: amemiya.naoyuki.6a@kyoto-u.ac.jp).

Color versions of one or more of the figures in this paper are available online at http://ieeexplore.ieee.org.

Digital Object Identifier will be inserted here upon acceptance.

II. Measurement and Analysis Methods

A. Multipole Magnetic Field Measurements [11]

We conducted multipole magnetic field measurements using the rotating pickup coil method. In this method, the pickup coil is rotated at a constant speed in the magnetic field at the center of the magnet, and the induced voltage generated by the change in the interlinkage magnetic flux is measured. The multipole components of the magnetic field are obtained using the Fourier series expansion of the measured induced voltage of the pickup coil. It is worth noting that the measurements obtained using this method have a low time resolution. Therefore, it is difficult to evaluate the time variation in the 10-s *step* described in the following section.

B. Numerical Electromagnetic Field Analyses [12]

In the numerical electromagnetic field analyses, finite element method with *T*-formulation, and thin-strip approximation was used. The equations solved in the analyses were as follows:

$$\nabla\times\left(\frac{1}{\sigma}\nabla\times\boldsymbol{n}T\right)\cdot\boldsymbol{n}+\frac{\partial}{\partial t}\frac{\mu_0 t_s}{4\pi}\cdot\left(\int_{S'}\left[\left\{(\nabla\times\boldsymbol{n}'T')\times\boldsymbol{r}\cdot\boldsymbol{n}\right\}/r^3\right]\mathrm{d}S'+\boldsymbol{B}_{\mathrm{ext}}\cdot\boldsymbol{n}\right)=0. \quad (1)$$

Template version 8.0d, 22 August 2017. IEEE will put copyright information in this area
See http://www.ieee.org/publications_standards/publications/rights/index.html for more information.

京都大学 KYOTO UNIVERSITY
A Self-archived copy in
Kyoto University Research Information Repository
https://repository.kulib.kyoto-u.ac.jp
京都大学学術情報リポジトリ KURENAI 紅 Kyoto University Research Information Repository

TABLE I
SPECIFICATIONS OF THE MAGNET AND THE COATED CONDUCTORS

Magnet	
Configuration	Split arrangement of 4 racetrack coils. Each pole is composed of 2 racetracks coils.
Distance between poles	55.4 mm
Inner / Outer radius	48 mm / 68.5 mm
Length of straight part	250.0 mm
Number of turns per racetrack coil	110
Designed dipole component of magnetic field	250 mT with 100 A
Temperature	30 K by conduction cooling
Coated conductor	
Manufacturer	SuperPower Inc. (SCS4050)
Width	4 mm
Thickness of coated conductor	0.093 mm
Thickness of superconductor layer	1.7 μm

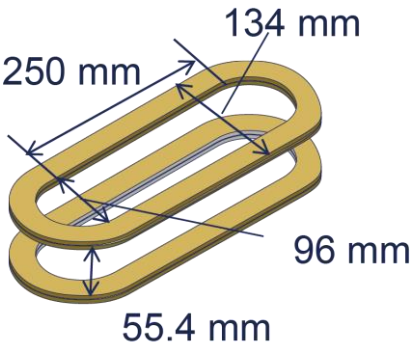

Fig. 1. Bird's eye view schematic of the coil used for the magnet

TABLE II
PARAMETERS OF EXCITATION PATTERNS

Pattern	Excitation pattern	Time of constant current (for patterns A and B) / current at steps (their durations) (for patterns C, D, and E)
A	Ramp-up to 100 A and hold	10 hours
B	Ramp-up to 150 A, ramp-down to 100 A, and hold	6 hours
C	Ramp-up to 150 A, ramp-down to 100 A, ramp-up to 150 A, repeat these	150 A, 125 A, 100 A (10 s) in ramp-down process
D	Ramp-up to 150 A, ramp-down to 50 A, ramp-up to 150 A, repeat these	150 A, 125 A, 100 A, 75 A, 50 A (10 s) in ramp-down process
E	Ramp-up to 150 A, ramp-down to 50 A, ramp-up to 150 A, repeat these	150 A (60 s) 125 A, 100 A, 75 A, 50 A (10 s) in ramp-down process

Here, T and T' are the magnitudes of the current vector potentials at the field point and source point, respectively. $\boldsymbol{n}$ and $\boldsymbol{n}'$ are normal vectors at the field point and source points, respectively, and $\boldsymbol{r}$ is a vector from the source point to the field point. t_s and σ are the thickness of the superconductor layer and its conductivity, respectively. S' is the area of the wide face of the

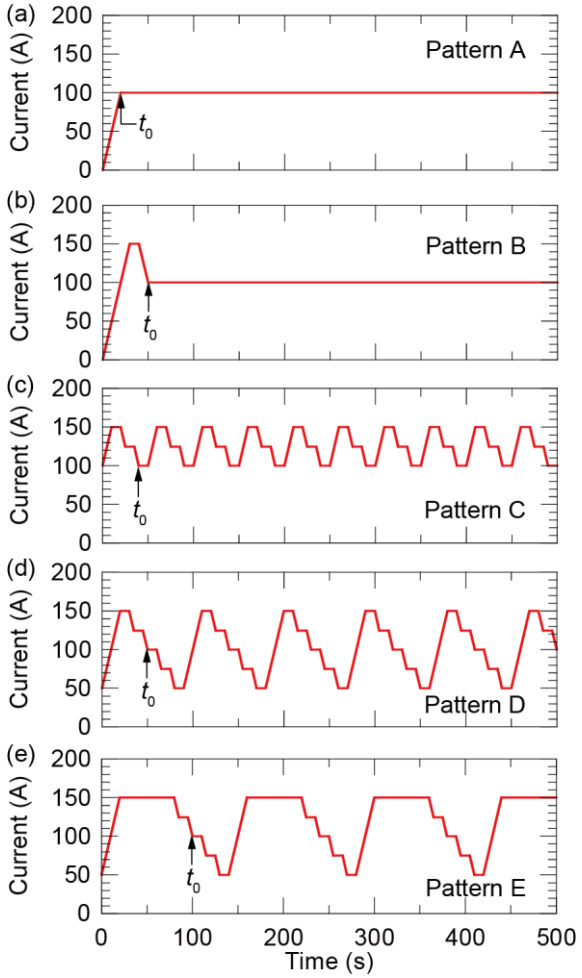

Fig. 2. Current profile of all excitation patterns. For patterns A and B, complete profile is shown. For patterns C, D, and E, one cycle of repeated excitation (from ramp-up to ramp-down) is shown. Ramp-up and ramp-down rate is 5 A/s.

superconductor layer of the coated conductors. To calculate σ, we used the measured electric field E–current density J characteristics, of the coated conductors used for the coil.

We applied hierarchical matrices to the analysis model to handle large-scale numerical electromagnetic field analyses.

III. MEASURED AND ANALYZED MAGNET AND CONDITIONS

Table I lists the specifications of the magnet and the coated conductors. Fig. 1 shows the bird's eye view schematic of the measured and analyzed magnet. The magnet was a dipole magnet with four racetrack coils. The coils are wound with coated conductors manufactured by SuperPower Inc. The magnet was cooled at 30 K by using cryocooler, and its critical current was approximately 250 A.

We used a stable power supply, with an output current drift in the order of ppm/hour. In this study, we set up five different excitation patterns, which could be classified into two categories: constant current excitation, and repeated excitation. The excitation parameters are listed in Table II, and their current profiles are presented in Fig. 2. It is worth noting that the

京都大学 KYOTO UNIVERSITY
A Self-archived copy in
Kyoto University Research Information Repository
https://repository.kulib.kyoto-u.ac.jp
京都大学学術情報リポジトリ KURENAI 紅 Kyoto University Research Information Repository

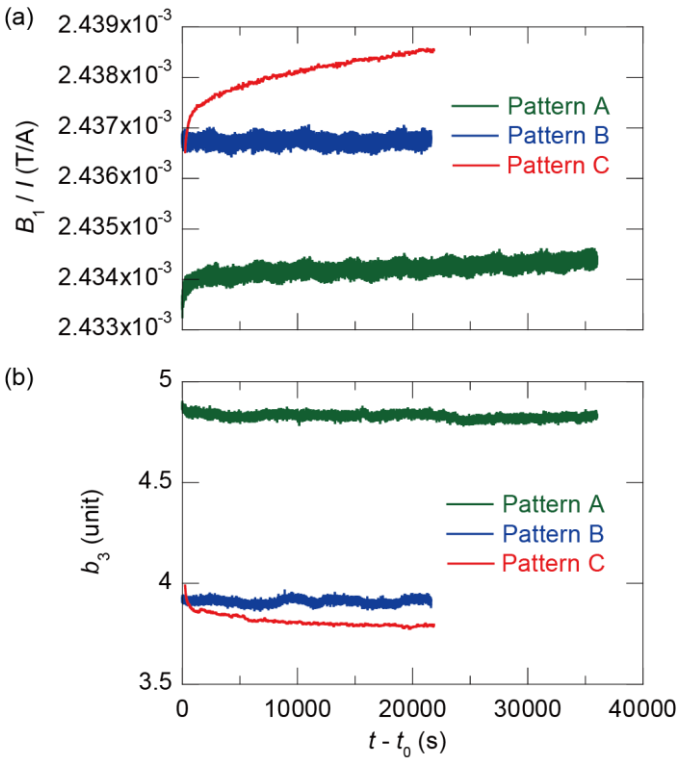

Fig. 3. Measured temporal evolution of multipole components of magnetic field at 100 A under excitation patterns A, B, and C: (a) dipole component B_1 of magnetic field normalized by transport current, and (b) sextupole coefficient b_3 of magnetic field, normalized by B_1 and then multiplied by 10^4. For pattern C, the averaged values of B_1 / I and b_3 in each step are plotted. t_0 of each pattern is denoted in Fig. 2.

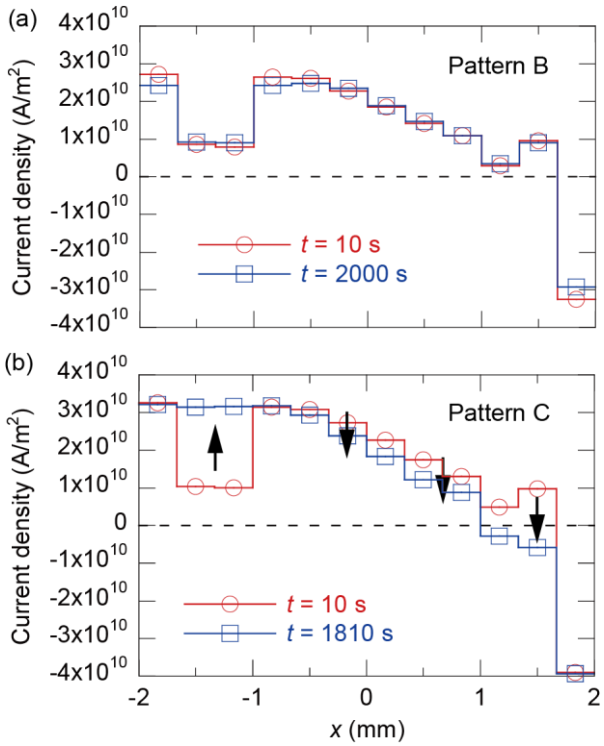

Fig. 4. Analyzed current density distribution across the width of the coated conductor at 100 A: (a) in pattern B and (b) in pattern C. The coated conductor at the center of the straight part of the innermost turn of the magnet is plotted. The negative x corresponds to the edge of the coated conductor closer to the center of the magnet.

magnet was warmed to approximately room temperature to eliminate the remnant magnetization after each excitation.

Under constant current excitation, the excitation was not repeated, and a constant current was supplied to the coil for a long time. The results under the constant current excitation served as references for those under the repeated excitations. In pattern A, the current was ramped up to 100 A, and kept constant for 10 h. In pattern B, the current was ramped up to 150 A, ramped down to 100 A, and then kept constant for 6 h. The ramp-up, and ramp-down rate of the current was 5 A/s.

In the repeated excitation, the ramp-up and ramp-down of the current were repeated for approximately 6 h. The current was kept constant for a short duration (10 s in patterns C and D, 60 s in pattern E) at the maximum current, which was called the flat-top. During the ramp-down process, we set multiple steps in which the current was temporally kept constant for 10 s. The current was ramped down to 100 A for patterns C, and 50 A for patterns D and E. The ramp-up, and ramp-down rate of the current was 5 A/s.

IV. Results and Discussions

A. Comparison of Drift of Magnetic Fields under Constant Current Excitation and Repeated Excitation

Fig. 3 shows the measured temporal evolution of the dipole, and sextupole components of the magnetic fields at 100 A under excitation patterns A, B, and C. For pattern C, the multipole components of the magnetic field were averaged at each 100-A step, and the time duration considered for the plot was 5 s after the start of each step. In Fig. 3(a), the dipole component of the magnetic field, $B_1(t)$ was normalized by the measured transport current $I(t)$. b_3 denotes the sextupole magnetic field coefficient, which was the sextupole component of the magnetic field, $B_3(t)$ normalized by $B_1(t)$, and then multiplied by 10^4. The initial time t = 0 s was defined as the time just after the current reached 100 A for patterns A and B, and as the time just after the current reached the first 100-A step for pattern C.

B_1 in pattern A drifted significantly, immediately after the current ramp-up, and continued to drift slowly thereafter. The decay of the magnetic field cannot be explained by using the critical state model. Contrarily, there was no significant drift of B_1 in pattern B. For b_3, there was no significant drift in either pattern A or B. For both B_1 and b_3, there was a difference in their magnitudes between patterns A and B. The method of raising the transport current above the operation current in pattern B is called the overshoot method, and it was reported to suppress the drift of the SCIFs, and reduce its magnitude [13, 14]. The overshoot method was also effective in the measured magnet, and a more stable magnetic field was observed under excitation pattern B.

Since the steps in pattern C were present during the ramp-down process, the current change was almost identical to pattern B till the first 100-A step, and the SCIF was consistent. However, the temporal variation of B_1 and b_3 thereafter were

京都大学 KYOTO UNIVERSITY
A Self-archived copy in
Kyoto University Research Information Repository
https://repository.kulib.kyoto-u.ac.jp
京都大学学術情報リポジトリ KURENAI 紅 Kyoto University Research Information Repository

TABLE III
FACTORS DETERMINING CURRENT DENSITY DISTRIBUTION IN COATED CONDUCTORS IN PATTERNS B AND C WITH DIFFERENT *E-J* CHARACTERISTICS

Pattern	Model for superconducting property	(1) Self-induced electromotive force due to change in shielding current	(2) Mutual-induced electromotive force due to change in magnetic field	(3) Non-linear resistance of superconductors
B	Critical state model	Exist	Not exist	Not exist
	Non-linear *E-J* model	Exist	Not exist	Exist
C	Critical state model	Exist	Exist	Not exist
	Non-linear *E-J* model	Exist	Exist	Exist

very different between patterns B and C. The drifts of B_1 and b_3 were more pronounced in pattern C.

The difference in the temporal evolution of B_1 and b_3 in Fig. 3 suggested that the relaxation of the shielding current in the coated conductors could be accelerated by repeated excitation. Fig. 4 shows the analyzed temporal change in the current density distribution across the coated conductor, for patterns B and C. In pattern B, the time variation of the current density distribution was not significant, as seen in Fig. 4(a). Contrarily, pattern C showed a clear change in the current density distribution over time. By repeated excitation, the current density increased in the region near the negative x edge, but decreased in the other region, as seen in Fig. 4(b). Thus, the magnetic flux density distribution as well as shielding current in the coated conductor was relaxed by repeated excitation. The change of B_1 and b_3 as well as current density distribution could not be explained by using the critical state model, but might be caused by the finite and non-linear *E-J* characteristics.

The factors determining current density distribution in coated conductors in patterns B and C with different models for superconducting property are summarized in Table III, and the flowchart for explanation of decay of shielding current in the repeated excitation with the non-linear *E-J* characteristics is shown in Fig. 5. The important difference between patterns B and C is the existence of (2) in Table III. High electric field remains at the tape edges by (2) at the beginning of the steps, which was induced by change of the magnetic field during ramp-down. By the high electric field, high current density appears at the tape edge. However, because integrated current density in tape cross section should be equal to the transport current, the current density at inside of tapes have to be decreased. Additionally, because there is large resistance at the tape edge derived from the non-linear *E-J* characteristics due to induced high electric field, the current density at the tape edges decays quickly. And then, the same phenomenon is observed in the step in the next ramp-down, and the relaxation of shielding current continues. Consequently, the fast decay of shielding currents is observed in repeated excitation. The relaxation of the shielding current was accelerated by repeated excitation, which could have caused the difference in the drift of the magnetic field seen in Fig. 3.

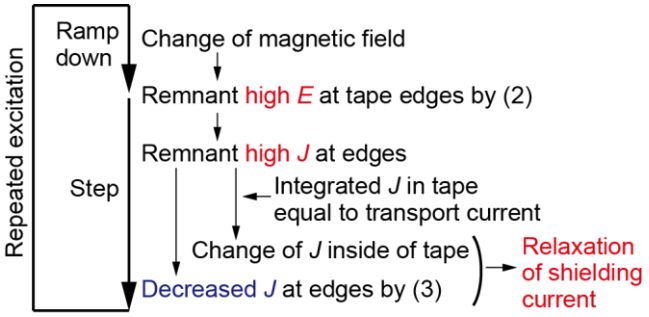

Fig. 5. Flowchart for explanation of fast decay of SCIF in pattern C with non-linear *E-J* characteristics.

B. Influence of Repeated Excitation Pattern on Drift of Magnetic Field

We compared the changes in the drift of the magnetic field for different repeated excitation patterns, specifically for the

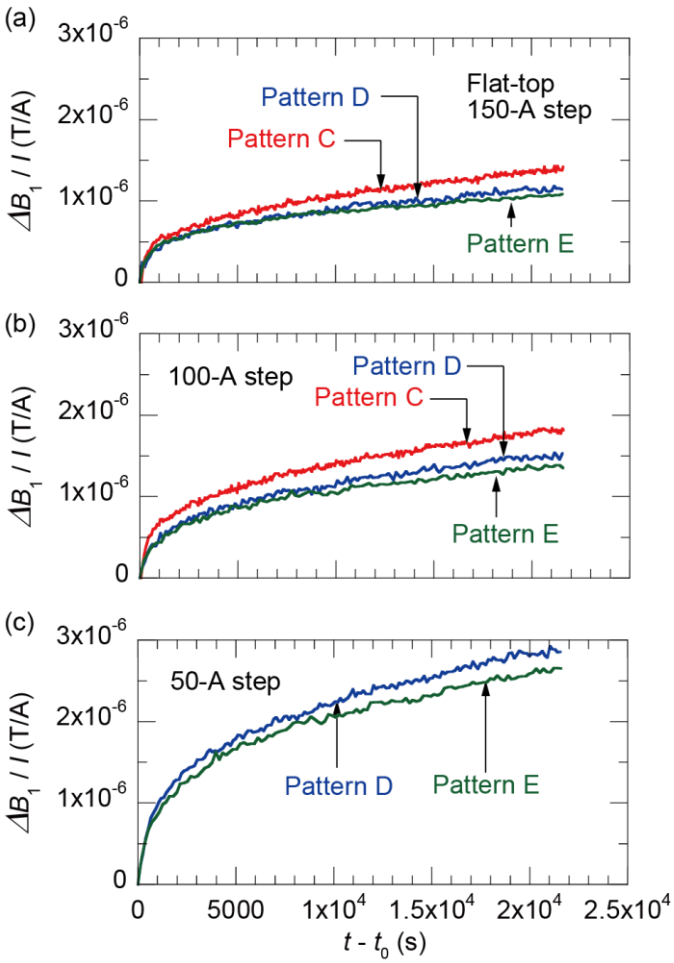

Fig. 6. Measured temporal evolution of ΔB_1 normalized by transport current, plotted against time under excitation patterns C, D, and E at (a) 150-A steps (flat-top), (b) 100-A steps, and (c) 50-A steps. Since there were no 50-A steps in pattern C, it was not plotted in (c). Each plot is the averaged value of ΔB_1 in each step. t_0 of each pattern is denoted in Fig. 2.

京都大学 KYOTO UNIVERSITY
A Self-archived copy in
Kyoto University Research Information Repository
https://repository.kulib.kyoto-u.ac.jp
京都大学学術情報リポジトリ KURENAI 紅 Kyoto University Research Information Repository

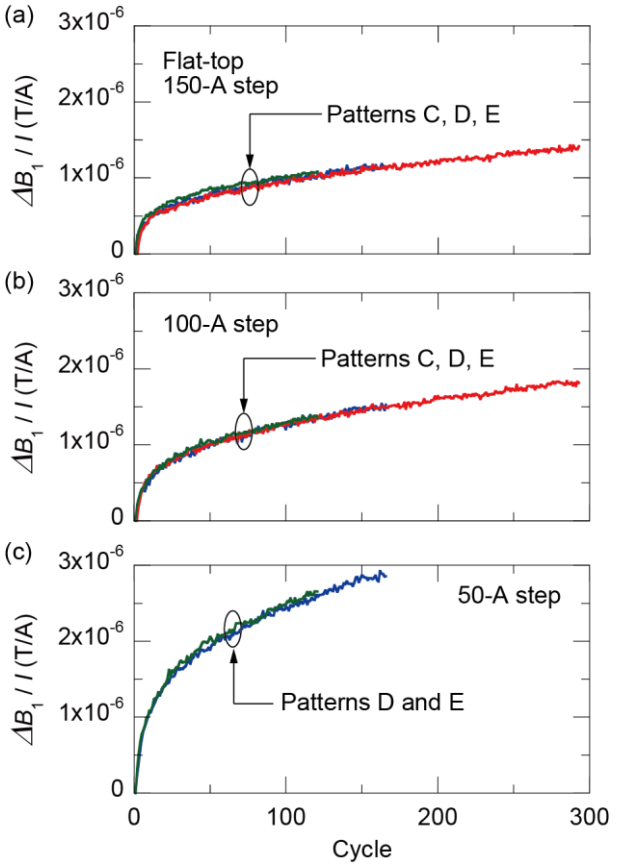

Fig. 7. Measured temporal evolution of ΔB_1 normalized by transport current, plotted against number of repetitions (cycles) under excitation patterns C, D, and E at (a) 150-A steps (flat-top), (b) 100-A steps, and (c) 50-A steps. Since there were no 50-A steps in pattern C, it was not plotted in (c).

minimum current, and the length of the flat-top. In this subsection, we focused on the drift of the dipole magnetic field component, B_1 caused by repeated excitation in flat-tops, 100-A steps, and 50-A steps. To discuss this, we used following ΔB_1:

$$\Delta B_1 = B_1 - B_{1,\mathrm{step}} \quad (2)$$

Here, $B_{1,\mathrm{step}}$ is the averaged B_1 in the first flat-top, or steps $B_{1,1\mathrm{st}}$, and B_1 is in arbitrary flat-top, or steps. ΔB_1 was plotted against time in Fig. 6 for patterns C, D, and E.

The drift of ΔB_1 was larger in patterns C, D, and E, in that order. For all patterns, there was a significant drift during the first 2,000 s, and the speed of the drift thereafter was almost constant. The relative magnitude of the drift during the six hours of repeated excitation was approximately 10^{-3}. Furthermore, the magnitude of the drift of B_1 in steps was less than 10^{-7} T/A, that was evaluated by numerical electromagnetic field analyses; hence, the drift of the SCIFs in each step was negligible in every pattern. Furthermore, the drift of ΔB_1 was smaller for steps with larger currents. This was attributed to the fact that the smaller the current, the larger the influence of the SCIF, thus indicating that the SCIF was generated in the direction cancelling the generated magnetic field in the magnet.

In Fig.7, the temporal evolution of ΔB_1 at each 150-A step (flat-top), 100-A step, and 50-A step is plotted against the number of repetitions. In all patterns, the temporal drift of ΔB_1 due to repeated excitation was in good agreement with each other. Therefore, the drift due to repeated excitation strongly depended on the number of repetitions rather than the elapsed time, from the start of the repeated excitation. This result implied that the drift of the SCIF of the magnet under repeated excitations could be predicted from the number of repetitions, thus suggesting the possibility of easy prediction using numerical electromagnetic field analyses.

V. Conclusion

We evaluated the temporal behavior of the magnetic field of a small dipole magnet wound with coated conductors operated under repeated excitation, using multipole magnetic field measurements and numerical electromagnetic field analyses. The drift of magnetic fields under repeated excitation was larger than that under constant current excitation, and was mainly dominated by the number of repetitions of excitation, and not by the time elapsed since the start of the repeated excitation. The poor stability was attributed to the acceleration of the diffusion of magnetic flux in the coated conductors caused by repeated excitation.

References

[1] H. Maeda and Y. Yanagisawa, “Recent Developments in High-Temperature Superconducting Magnet Technology (Review),” *IEEE Trans. Appl. Supercond.*, vol. 24, no. 3, Jun. 2014, Art no. 4602412.

[2] L. Rossi et al., “The EuCARD-2 Future Magnets European Collaboration for Accelerator-Quality HTS Magnets,” *IEEE Trans. Appl. Supercond.*, vol. 25, no. 3, Jun. 2015, Art no. 4001007.

[3] X. Wang et al., “Development and performance of a 2.9 Tesla dipole magnet using high-temperature superconducting CORC® wires,” *Supercond. Sci. Technol.*, vol. 34, no. 1, Dec. 2020, Art no. 015012.

[4] C. S. Myers, M. D. Sumption and E. W. Collings, "Magnetization and Flux Penetration of YBCO CORC Cable Segments at the Injection Fields of Accelerator Magnets," *IEEE Trans. Appl. Supercond.*, vol. 29, no. 5, Aug. 2019, Art no. 4701105.

[5] N. Amemiya et al., "AC Loss and Shielding-Current-Induced Field in a Coated-Conductor Test Magnet for Accelerator Applications under Repeated Excitations," *IEEE Trans. Appl. Supercond.*, vol. 30, no. 4, Jun. 2020, Art no. 4004105.

[6] N. Amemiya and K. Akachi, “Magnetic field generated by shielding current in high T_c superconducting coils for NMR magnets,” *Supercond. Sci. Technol.*, vol. 21, no. 9, Jun. 2008, Art no. 095001.

[7] N. Amemiya, Y. Sogabe, M. Sakashita, Y. Iwata, K. Noda, T. Ogitsu, Y. Ishii, and T. Kurusu, “Magnetisation and field quality of a cosine-theta dipole magnet wound with coated conductors for rotating gantry for hadron cancer therapy,” *Supercond. Sci. Technol.*, vol. 29, no. 2, Dec. 2015, Art no. 024006.

[8] L. Bortot, M. Mentink, C. Petrone, J. Van Nugteren, G. Kirby, M. Pentella, A. Verweij, and S. Schöps, “Numerical analysis of the screening current-induced magnetic field in the HTS insert dipole magnet Feather-M2.1-2,” *Supercond. Sci. Technol.*, vol. 33, no. 12, Oct. 2020, Art no. 125008.

[9] G. Baek, J. Kim, S. Han, Y. S. Yoon, S. Lee and T. K. Ko, "Effect of Screening Current Induced Field on Field Quality of an Air-Core HTS Quadrupole Magnet," *IEEE Trans. Appl. Supercond.*, vol. 30, no. 4, Jun. 2020, Art no. 4602304.

[10] Y. Iwata et al., “Development of a superconducting rotating-gantry for heavy-ion therapy,” *Nucl. Instrum. Methods Phys. Res.*, B, vol. 317, no. 15, Dec. 2013, pp. 793-797.

[11] N. Amemiya, H. Otake, T. Sano, T. Nakamura, T. Ogitsu, K. Koyanagi, and T. Kurusu, “Temporal behaviour of multipole components of the magnetic field in a small dipole magnet wound with coated conductors,” *Supercond. Sci. Technol.*, vol. 28, no. 3, Jan. 2015, Art no. 035003.

[12] T. Mifune, N. Tominaga, Y. Sogabe, Y. Mizobata, M. Yasunaga, A. Ida, T. Iwashita, and N. Amemiya, “Large-scale electromagnetic field

京都大学 KYOTO UNIVERSITY
A Self-archived copy in
Kyoto University Research Information Repository
https://repository.kulib.kyoto-u.ac.jp
京都大学学術情報リポジトリ KURENAI 紅 Kyoto University Research Information Repository

analyses of coils wound with coated conductors using a current-vector-potential formulation with a thin-strip approximation," *Supercond. Sci. Technol.*, vol. 32, no. 9, Jul. 2016, Art. no. 094002.

[13] T. Hemmi, N. Yanagi, G. Bansal, K. Seo, K. Takahata, and T. Mito, "Electromagnetic behavior of HTS coils in persistent current operations," *Fusion Eng. Des.*, vol. 81, no. 20–22, Nov. 2006, pp. 2463–6.

[14] M. Tsuda, R. Takano, H. Miura, D. Miyagi, T. Matsuda and S. Yokoyama, "Suitable Excitation Condition in Overshooting Process for Suppressing Magnetic Field Attenuation in Y-Based Coated Conductor Coils," *IEEE Trans. Appl. Supercond.*, vol. 27, no. 4, Jun. 2017, Art no. 8200305.